Mutations in *INPP5K* Cause a Form of Congenital Muscular Dystrophy Overlapping Marinesco-Sjögren Syndrome and Dystroglycanopathy

Daniel P.S. Osborn,[1] Heather L. Pond,[2] Neda Mazaheri,[3,4] Jeremy Dejardin,[1] Christopher J. Munn,[5] Khaloob Mushref,[2] Edmund S. Cauley,[2] Isabella Moroni,[6] Maria Barbara Pasanisi,[6,7] Elizabeth A. Sellars,[8] R. Sean Hill,[9,10] Jennifer N. Partlow,[9,10] Rebecca K. Willaert,[11] Jaipreet Bharj,[1] Reza Azizi Malamiri,[12] Hamid Galehdari,[3,4] Gholamreza Shariati,[4,13] Reza Maroofian,[1,14] Marina Mora,[7] Laura E. Swan,[5] Thomas Voit,[15] Francesco J. Conti,[15] Yalda Jamshidi,[1,16,*] and M. Chiara Manzini[2,16,*]

Congenital muscular dystrophies display a wide phenotypic and genetic heterogeneity. The combination of clinical, biochemical, and molecular genetic findings must be considered to obtain the precise diagnosis and provide appropriate genetic counselling. Here we report five individuals from four families presenting with variable clinical features including muscular dystrophy with a reduction in dystroglycan glycosylation, short stature, intellectual disability, and cataracts, overlapping both the dystroglycanopathies and Marinesco-Sjögren syndrome. Whole-exome sequencing revealed homozygous missense and compound heterozygous mutations in *INPP5K* in the affected members of each family. *INPP5K* encodes the inositol polyphosphate-5-phosphatase K, also known as *SKIP* (skeletal muscle and kidney enriched inositol phosphatase), which is highly expressed in the brain and muscle. INPP5K localizes to both the endoplasmic reticulum and to actin ruffles in the cytoplasm. It has been shown to regulate myoblast differentiation and has also been implicated in protein processing through its interaction with the ER chaperone HSPA5/BiP. We show that morpholino-mediated *inpp5k* loss of function in the zebrafish results in shortened body axis, microphthalmia with disorganized lens, microcephaly, reduced touch-evoked motility, and highly disorganized myofibers. Altogether these data demonstrate that mutations in *INPP5K* cause a congenital muscular dystrophy syndrome with short stature, cataracts, and intellectual disability.

Congenital muscular dystrophy (CMD) encompasses a group of disorders characterized by muscle weakness and progressive loss of muscle mass and function, presenting at birth or infancy.[1,2] Multiple forms of CMDs are also associated with cerebral and ocular phenotypes, suggesting common mechanisms affecting development of the muscle, brain, and eye. For these syndromic forms, gene identification studies have primarily pointed to a molecular mechanism involving interactions between cells and the surrounding extracellular matrix (ECM).[3] Mutations in up to 19 glycosyltransferases and accessory proteins involved in the glycosylation of the transmembrane glycoprotein dystroglycan (*DAG1* [MIM:128239]) lead to a spectrum of CMDs termed dystroglycanopathies.[4,5] Dystroglycanopathy-associated genes function in the endoplasmic reticulum (ER) and/or Golgi apparatus to regulate dystroglycan glycosylation. Genetic and function studies have shown that glycans are critical to control normal tissue development in the brain, eye, and muscle, via interactions with the ECM.[5] The most severe forms of dystroglycanopathy present with CMD associated with lissencephaly (smooth brain) and a variety of eye malformations affecting both the retina and the anterior chamber (e.g., cataracts, glaucoma), but multiple case subjects have only CMD with intellectual disability and more subtle brain findings.[6,7]

Marinesco-Sjögren syndrome (MSS [MIM:248800]) is a form of myopathy with a similar constellation of findings including muscle involvement, intellectual disability, cataracts, brain MRI findings, and other signs of central nervous system (CNS) involvement.[8,9] Cerebellar atrophy is often considered the most prominent neuroradiologic finding in MSS, but it is not an obligatory finding.[10] The clinical overlap can therefore make it difficult to distinguish between syndromic CMDs and MSS. MSS is also considered to be a clinically and genetically heterogeneous disorder with approximately 70% of MSS-affected case subjects harboring mutations in *SIL1* (MIM: 608005).[8]
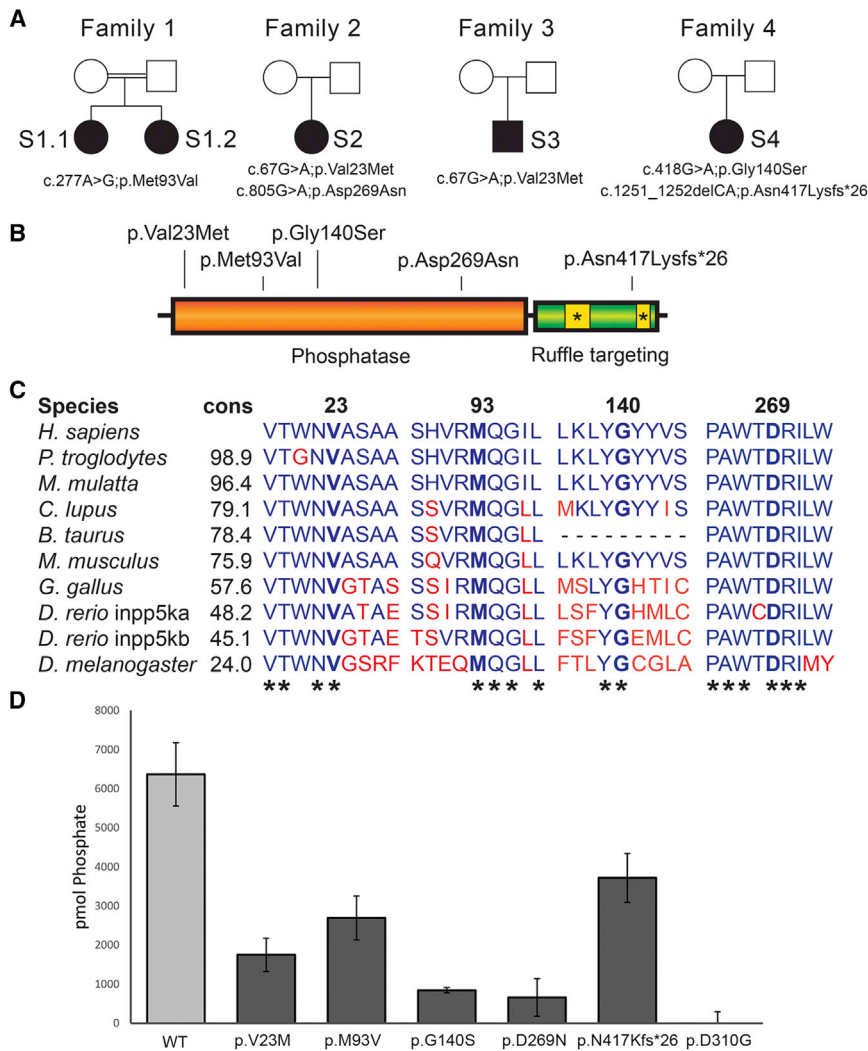
Figure 1. Mutations in *INPP5K* Severely Disrupt Protein Function

(A) Pedigrees of families 1 to 4 where five autosomal-recessive alleles in *INPP5K* have been identified by exome sequencing.

(B) Four missense mutations are localized to the phosphatase domain in INPP5K, while a C-terminal frameshift affects the last actin ruffle targeting domain.

(C) Protein conservation in the four INPP5K amino acids altered by the identified missense mutations. Percent conservation (cons) to the human gene is shown and asterisk (*) indicates conservation across all species listed.

(D) Phosphatase activity was measured by using malachite green dye to detect GST-INPP5K-mediated phosphate release in the presence of the soluble lipid substrate $PI(4,5)P_2$ diC_8, showing that all reported mutations compromise the enzymatic activity of INPP5K. Results of three independent experiments were presented as mean ± standard deviation. See Table 1 for numeric values.

SIL1 acts as a nucleotide exchange factor for heat shock protein family A member 5 (HSPA5) (also known as GRP78 [glucose-related protein 78] or BiP [immunoglobulin binding protein]), an essential regulator of ER function; the identification of these mutations has led to the suggestion that MSS is a disorder of protein biosynthesis or processing in the ER.[11]

In this report, we present five individuals from four families diagnosed with a syndrome overlapping both the dystroglycanopathy and the MSS spectrum with recessive mutations in inositol polyphosphate-5-phosphatase K (*INPP5K* [MIM:607875]) (Figure 1). INPP5K belongs to a family of phosphatidylinositol (PI) phosphatases responsible for removing the phosphate on position 5 of the inositol ring leading to $PI(3,4)P_2$ from $PI(3,4,5)P_3$ and P4P from $PI(4,5)P_2$. Also known as skeletal muscle and kidney-enriched inositol phosphatase (*SKIP*), *INPP5K* is highly expressed in the developing and adult brain, eye, and muscle.[12–14] It is primarily localized to the ER, and it can form a complex with HSPA5/BiP to regulate insulin receptor signaling at actin ruffles on the plasma membrane by acting as a negative regulator of phosphatidylinositol-3-kinase (PI3K) signaling,[15] suggesting a possible overlap with the function of the MSS-associated gene *SIL1*.

In agreement with the Declaration of Helsinki, informed consent for genetic and biochemical studies was obtained from all study participants or their guardians under the authority of the George Washington University Internal Review Board and the Narges Medical Genetics and Prenatal Diagnosis Laboratory. Subjects 1.1 and 1.2 (S1.1 and S1.2; Figure 1A, Table 1) are two affected sisters (7 and 13 years old) born of an Arabian consanguineous family in Iran, who were initially diagnosed with muscle atrophy and global developmental delay. Both were born without complications, and early development was normal with the exception of delayed walking from 18 months after a period of occupational therapy. Both sisters experienced febrile seizures in infancy (9 months) and early childhood (2 years), and routine interictal electroencephalography in the elder sister was normal. They displayed difficulty rising from a squatting position, impaired toe-standing, and unsteady gait. At the age of 2 years the elder sister began to show hypotonicity that progressed to spasticity including diffuse loss of muscle bulk, exaggerated deep tendon reflexes, positive pyramidal signs, and fatty infiltration resulting in frequent falls, toe walking, spastic gait, and pronounced hyperlordosis. Neither sister can climb stairs without support. After orthopedic surgery, the elder sister uses a wheelchair and muscle biopsy showed myogenic atrophy. Electromyogram (EMG) report also showed the presence of myopathy involving both her lower limbs, with more involvement of the proximal

Table 1. Clinical Features of Individuals with Biallelic *INPP5K* Mutations

Subject	S1.1	S1.2	S2	S3	S4
Protein change	p.Met93Val	p.Met93Val	p.Val23Met; p.Asp269Asn	p.Val23Met	p.Gly140Ser; p.Asn417Lysfs*26
% WT function	42% ± 9%	42% ± 9%	27% ± 7%; 10% ± 8%	27% ± 7%	13% ± 1%; 58% ± 10%
Ethnic origin	Iranian-Arab	Iranian-Arab	Italian	Italian	European American
Sex	F	F	F	M	F
Current age	13 y	7 y	31 y	21 y	17 y
Short stature	+	+	+	+	+
Cataracts	−	+	+	−	+
Strabismus	+	+	−	−	+
Spine hyperlordosis	+	+	−	+	−
Muscle weakness	+	+	+	+	+
CK	1,041 U/L	1,184 U/L	elevated	>1,000 U/L	elevated
EMG	myopathic changes	NA	myopathic changes	myopathic changes	NA
Muscle biopsy	myogenic atrophy	NA	dystrophic; reduced α-DG	dystrophic; reduced α-DG	NA
Spasticity	+	+	+/−	−	+
Mobility	wheelchair-bound	assisted walking	wheelchair-bound	wheelchair-bound	ambulatory
Intellectual disability	moderate/severe	moderate/severe	moderate/severe	moderate	moderate
Seizures	+	+	+	−	−
Microcephaly	borderline	+	−	+	+
MRI	normal	NA	brain atrophy	normal	normal

Abbreviations are as follows: WT, wild type; y, years; NA, not assessed; α-DG, α-dystroglycan.

muscles. Both sisters have increased serum creatine kinase (CK), aldolase, and alkaline phosphatase levels. They have moderate to severe intellectual disability (ID), both attending special schools. Brain magnetic resonance imaging (MRI) of S1.1 was normal at the ages of 8 and 13. Both sisters have short stature, microcephaly, and impaired speech. Variable clinical features include bilateral cataracts in S1.2.

Whole-exome sequencing (see Table S1 for details) was performed on S1.1, focusing on the identification of potentially deleterious rare homozygous variants due to the presence of multiple large regions of homozygosity. Thirteen candidate genes were identified with homozygous missense mutations (Table S2). A homozygous variant in *INPP5K* (GenBank: NM_016532; Table S3) was identified within an 8-Mb region of homozygosity (c.277A>G [p.Met93Val]) (Figures 1A and 1B). Sanger sequencing confirmed that both affected children were homozygous for this variant and each parent was heterozygous for the variant. The variant is unique in an in-house dataset of 450 geographically matched individuals sequenced by exome and is not represented in the Greater Middle Eastern Variome,[16] in 60,706 individuals in the Exome Aggregation Consortium (ExAC) Browser,[17] or in 141,353 individuals in the Genome Aggregation Database (gnomAD). This mutation affects a highly conserved residue (Figure 1C) and is predicted to be pathogenic by multiple prediction tools (SIFT = 0.01; CADD = 22.7)[18] (Table S3).

Subjects 2 (S2) and 3 (S3) were simplex cases originating from southern Italy. S2 (Figure 1A, Table 1) is 31 years old and was referred with a diagnosis of CMD as a child. She was born at term with low birth weight and presented with motor and cognitive delay since early infancy. At 2 years of age, she underwent surgery for bilateral cataracts. Upon neuromuscular examination at age 5, she was able to walk independently, but her upper limbs were hypotonic and hypotrophic with no tendon reflexes and her lower limbs were slightly hypertonic with brisk tendon reflexes. CK and aldolase levels were reported as higher than normal. EMG revealed myopathic changes with normal sensory and motor conduction velocities. A biopsy of the quadriceps muscle showed neuromyogenic changes. Fiber diameter was variable, with several small rounded or wedge-shaped fibers, mildly increased perymisial connective tissue, rare centrally located nuclei, and a few degenerating and regenerating fibers (H&E staining, Figure 2A). α-dystroglycan immunohistochemistry using either the VIA4-1 or IIH6 antibody (Millipore) showed reduced protein glycosylation on fiber surfaces (Figure 2C). Dystrophin-associated glycoproteins and laminin-α2 were normally expressed (not shown). In addition
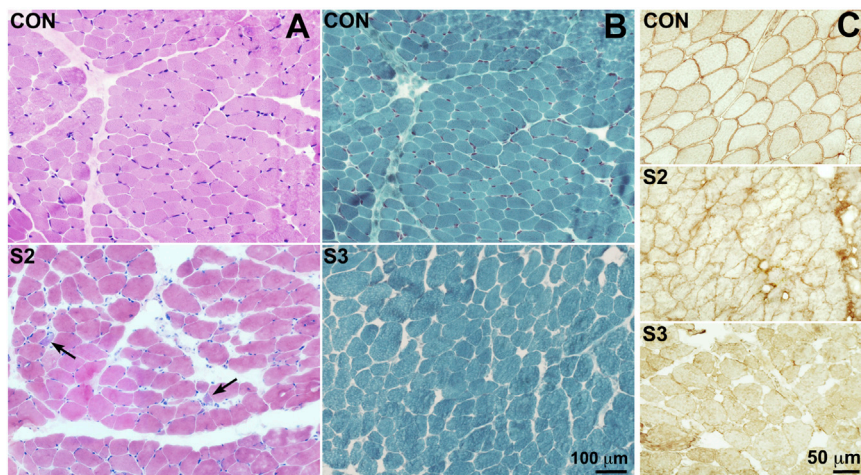
Figure 2. Muscular Dystrophy and Loss of Dystroglycan Glycosylation in Subjects S2 and S3

(A and B) Haematoxylin and eosin (H&E) staining (A) from normal control subject (con) and subject S2 and Gomori trichrome staining (B) from control (con) and subject S3. Both biopsies show great fiber size variability, and increased perimysial connective tissue and regenerating fibers are indicated by arrows in S2. Scale bar represents 100 μm.

(C) Immunostaining of α-dystroglycan glycosylation in muscle biopsies from S2 and S3, showing reduced and irregular protein expression in the affected individuals compared to the control subject (con). Scale bar represents 50 μm.

to the neuromuscular phenotype, she presented with dysmorphic features: short stature, thin hair, globular nose, and micrognathism, plus skeletal anomalies such as 13 ribs and scoliosis. A cerebral CT showed an elongated (dolichocephalic) skull, with underdevelopment of both cortex and white matter of cerebral hemispheres. She was treated for focal seizures until she was 10 years old. A brain MRI, performed at age 18 years, showed an anomaly of the craniovertebral junction (odontoid process in the foramen magnum) and enlarged lateral ventricles and subarachnoid spaces, suggesting progressive brain atrophy. During follow-ups, the subject's clinical features remained stable. She presents with moderate-severe ID without speech deficits and is very sociable. At 22 years of age she could still walk independently, but needed handrail support when going up and down stairs. Strength evaluation showed moderate proximal weakness of upper limbs and moderate-severe proximal and distal weakness of lower limbs with initial retractions of adductor muscles and Achilles tendons. Due to a fall resulting in a femur fracture at age 28, she is now wheelchair-bound.

S3 (Figure 1A, Table 1) is a 21-year-old male who also presented with delayed psychomotor development at 23 months after an uneventful pregnancy and delivery. Neurological examination at 3 years of age identified marked axial and limb hypotonia with proximal upper and lower limb weakness, marked lumbar hyperlordosis, and areflexia. Gower's sign was positive. CK was elevated often above 1,000 U/L and muscle biopsy showed neuromyogenic changes. A mild increase of perimysial connective tissue was noted with variable fiber size with hyper-, hypo-, and atrophic fibers, a few centrally located nuclei, split fibers, rare degenerating fibers, and small type groupings (Gomori trichrome staining, Figure 2B). α-dystroglycan immunohistochemistry showed reduced glycosylation expression on fiber surfaces (Figure 2C), while dystrophin, dystrophin-associated glycoproteins, and laminin-α2 were normally expressed. He was moderately dysmorphic with an elongated face. Mild ID and microcephaly were noted, but brain MRI was normal. During subsequent years

muscle weakness slowly worsened with loss of autonomous gait at age 12. No cardiac impairment was noticed at echocardiographic examinations, while a mild restrictive respiratory deficiency was noticed since adolescence. No eye involvement was reported until the last visit at age 21.

S2 and S3 underwent exome sequencing as part of a cohort of Italian case subjects with CMD with variable brain abnormalities and cognitive deficits (see Table S1 for details on exome). Exomes were filtered using custom SQL queries for rare (<0.5% frequency in the ExAC Browser for both total and non-Finnish European populations) and likely pathogenic (missense, splicing, or truncating) variants.[19] Remaining variants were visually analyzed on the Integrative Genomics Viewer (IGV),[20] leading to three candidate genes in S2 and three candidates in S3 (Table S2). Both individuals had biallelic missense variants in *INPP5K* (Figures 1A and 1B). S2 carries compound heterozygous transitions c.67G>A (p.Val23Met) and c.805G>A (p.Asp269Asn), while S3 is homozygous for c.67G>A (Table S3). Both variants affect conserved residues (Figure 1C), found in less than 1:100,000 alleles in the ExAC and gnomAD browsers and are predicted to be pathogenic (p.Val23Met: SIFT = 0; PolyPhen2 = 1; CADD = 16.7; p.Asp269Asn: SIFT = 0; PolyPhen2 = 1; CADD = 34) (Table S3).

Finally, subject 4 (S4, Figure 1A, Table 1) originated from the United States and was referred to us via GeneMatcher[21,22] after clinical exome sequencing in the trio (proband and parents). She is a 17-year-old female who presented in early childhood with delay in reaching motor and cognitive developmental milestones. She walked independently at 18 months. She did not babble until age 3 and had phrases at age 4. Bilateral cataracts were identified at 2 years of age and surgically corrected. Since childhood she had upper and lower limb hypotonia, leading to balance problems and frequent falls. CK is elevated above 1,000. Currently, she has an appreciable loss of muscle mass in her hands and feet. She toe walks and fatigues easily. EMG at 16 years of age was normal. A muscle biopsy has not been performed. She has short

stature for which she was treated with growth hormone. Other findings include hirsutism, microcephaly, and moderate ID. Brain MRI at age 16 was normal. Clinical exome sequencing was performed by GeneDX using proprietary capture chemistry (Table S1 for details). Further analysis identified *INPP5K* as the gene most likely to harbor the responsible pathogenic variants. S4 carries a likely pathogenic transition and a small deletion in compound heterozygosity, c.418G>A (p.Gly140Ser; SIFT = 0; PolyPhen2 = 1; CADD = 28.6) and c.1251_1252delCA (p.Asn417Lysfs*26) (Figures 1A and 1B). The missense variant alters a conserved residue and is extremely rare; the deletion is not found in ExAC and gnomAD browsers (Table S3).

In summary, all individuals with likely pathogenic biallelic mutations in *INPP5K* present with myopathic findings and elevated CK, short stature, motor and cognitive developmental delay since early infancy, and moderate-severe ID. Cataracts were present in S1.1, S2, and S4, but not S1.1's sibling S1.2, showing variability even within the same family. While no ataxia or cerebellar atrophy was noted, this presentation is reminiscent of MSS and could fall in the larger MSS spectrum.[23] In addition, a reduction in dystroglycan glycosylation in S2 and S3 suggest an overlap with less severe forms of dystroglycanopathies, where CMD is present with cataracts and ID.[6,7] Similar cases of merosin-positive CMD with cataracts and ID have been previously reported,[24,25] also suggesting that this disorder may represent a distinct clinical entity.

Since the identified variants are either missense or late truncations, we sought to determine their impact on protein function by performing phosphatase activity assays. GST-tagged full-length *INPP5K* constructs (wild-type and mutants) were assayed for their activity against 135 mM PtdIns(4,5)P$_2$diC8 soluble lipid substrate in phosphatase assay buffer (50 mM Tris-HCl [pH 7.5], 150 mM NaCl, 10 mM MgCl$_2$). Free phosphate was measured using the malachite green assay kit (Echelon Biosciences) and calibrated against standards according to the manufacturer's instructions. To minimize variability between purifications, all constructs were freshly prepared and purified in parallel for each experiment, and beads used in the assay were afterward run on Coomassie gels to confirm equal protein loading. We found that when compared to a phosphatase-dead construct (p.Asp310Gly), p.Gly140Ser and p.Asp269Asn had almost no enzymatic activity, while p.Val23Met and p.Met93Val retained 27% and 42% activity, respectively. The C-terminal frameshift deletion p.Asn417Lysfs*26, which is located outside of the phosphatase domain, was the least severely disrupted (57% activity in this assay) (Figure 1D). Both S1.1/2 and S3 are homozygous for variants that only partially reduce phosphatase activity of INPP5K, but analysis of more case subjects will be necessary to establish genotype/phenotype correlation.

To explore the role of *INPP5K* during early development, we targeted *inpp5k* in the zebrafish embryo using antisense morpholino oligonucleotides (MOs, GeneTools, LLC). Teleost fish underwent a genome duplication event, leading to approximately 30% of genes having a paralog.[26] *inpp5k* is present in two copies in the zebrafish genome: *inpp5ka* and *inpp5kb*. Alignment of both homologs indicate that *inpp5ka* is more similar to *INPP5K* (Figure S1), suggesting that it is the closest ortholog of the human gene. In addition, quantitative PCR expression analysis in the zebrafish embryo indicated that *inpp5ka* expression is, respectively, 7-fold and 16-fold higher than *inpp5kb* at 1 and 2 days post fertilization (dpf) (Figure S1B). MOs were designed by two independent groups to target both the start site (translation-blocking) and splicing of the *inpp5ka* and *b* mRNA, leading to four independent MOs being tested for each gene (Table S4, Figures 3 and S2–S4). Experiments were also performed on two independent strains, TupLF and AB.

Injections of *inpp5ka* MOs in the fertilized oocyte resulted in a striking phenotype in zebrafish embryos and larvae, which featured microphthalmia, microcephaly, curved and shortened body, and reduced touch-evoked motility (Figures 3A and S2–S4, Movies S1, S2, S3, S4, and S5). This phenotype was consistent across all *inpp5ka* MOs injections and in the *inpp5ka* and *b* double morphant, while *inpp5kb* MOs alone showed very mild phenotypes (Figures S2A–S2D and S4). It is not uncommon for one gene in a pair of duplicated orthologs to lose its function or be silenced.[27] Therefore, all subsequent analysis was performed on *inpp5ka* morphants to reduce as much as possible the amount of MO injected in the embryos and avoid non-specific effects. *inpp5ka* morphant phenotypes could be significantly improved by co-injection of 200 pg of capped human *INPP5K* mRNA, while injection of *INPP5K* mRNA alone had no effect (Figures S2E and S2F).

Examination of the eye by wax sectioning followed by H&E staining showed that in morphants eyes are orientated downward, as indicated by the position of the lens (Figure 3B). At 3 dpf the lens organizes in a cellular cortex and an acellular nucleus.[28] α-crystallin (zl-1; Zebrafish International Resource Center) immunostaining in axial sections of the *inpp5ka* morphant showed that the lens cortex was disorganized and cell nuclei were present in the center of the lens nucleus, leading to a phenotype reminiscent of congenital cataracts (Figure 3C).

A birefringence assay using polarized light to image the densely packed and highly organized nature of muscle fibers of control embryos showed that knockdown of *inpp5ka* caused a substantial reduction in birefringence (Figure 3D), suggesting muscle fiber disorganization. To better evaluate skeletal muscle structure, phalloidin (Molecular Probes) was used to mark filamentous actin (F-actin) in sarcomeres. Control embryos display densely packed, organized muscle fibers in the trunk of the zebrafish embryo (Figure 3E). *inpp5ka* morphants showed sparser, disorganized myofibers, with the appearance of "wavy fibers" (Figure 3E). As the role of INPP5K has not been previously characterized, we investigated its potential

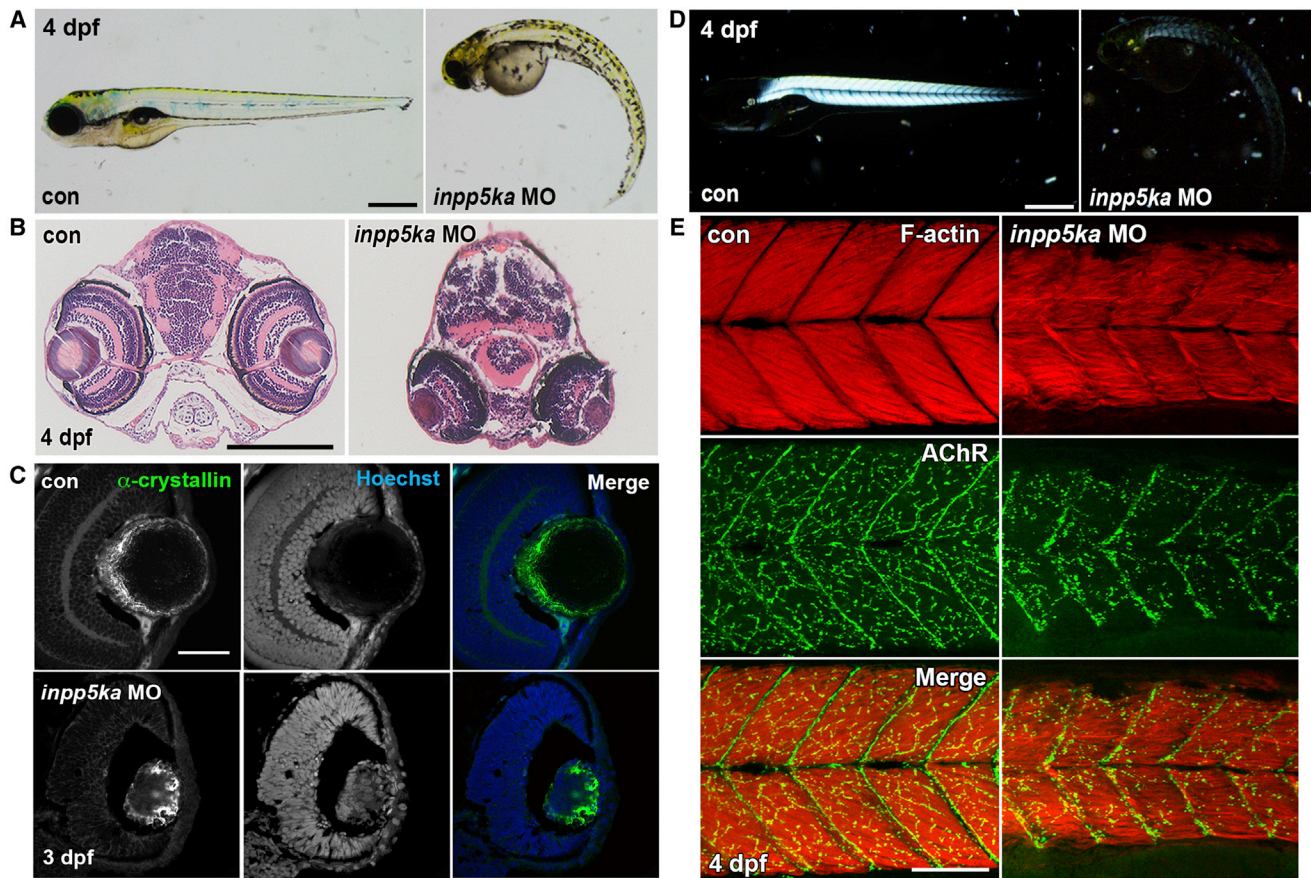**Figure 3. Knockdown of *inpp5ka* in Zebrafish Causes Defective Eye Development and Muscle Formation**
(A) General morphological abnormalities were observed in *inpp5ka* morphant embryos at 4 dpf, compared to control morpholino (MO) or uninjected control age-matched embryos. Scale bar represents 500 μm.
(B) Aberrant eye development was observed in *inpp5ka* morphant wax sections stained with H&E; eyes were observed reduced in size and downwardly oriented. Scale bar represents 200 μm.
(C) Structural analysis of the lens, by staining for α-crystallin, identifies disorganization in *inpp5ka* morphant embryos. In addition, abnormal medial nuclei retention was observed in *inpp5ka* morphant lens, as marked by DNA stain Hoechst. Scale bar represents 50 μm.
(D) Birefringence of *inpp5ka* morphant embryos reveals decreased muscle integrity compared to uninjected or control MO-injected embryos at 4 dpf. Scale bar represents 200 μm.
(E) Analysis of muscle fiber and neuromuscular junction formation using Phalloidin (Red, F-actin) and alpha-Bungarotoxin (Green, AChR), respectively, reveals misaligned myofibers and reduced NMJ arborization in morphants. Scale bar represents 100 μm.

role in the formation of neuromuscular junctions (NMJs). Analysis of NMJs, by targeting the acetylcholine receptors (AChR) using the high-affinity fluorophore-conjugated alpha-Bungarotoxin (Molecular Probes), reveals reduced synaptic formation in the skeletal muscle of *inpp5ka* knockdown embryos (Figure 3E). Thus, *inpp5ka* is required for appropriate formation of skeletal muscles and NMJs.

Finally, transmission electron microscopy (TEM) was used to expose sarcomeric assembly defects consistent with reduced motility in the morphants (Figure 4A). While control embryos display clearly defined electron dense anisotropic (A-bands) and less dense isotropic (I-bands) bands, the morphants have undefined A- and I-bands (Figure 4B). Sarcomere length is shorter in *inpp5ka* knockdown embryos, compared to control MO-injected or uninjected embryos, a phenotype normally associated with contracted sarcomeres. In addition, myofibrils are loosely packed with a disorganized arrangement in morphants.

Triads, consisting of T-tubules and sarcoplasmic reticulum (SR), are required for sarcomeric contraction. Knockdown of *inpp5ka* results in triads that are on average half the size of those in control embryos (Figures 4C–4E), a possible feature of an exhausted SR.[29] Muscular dystrophy phenotypes are associated with detachment of myofibers at somite borders.[30] We analyzed muscle fiber attachment at the somite borders in knockdown and control embryos (Figure 4C). Control embryos showed well-defined attachments to the myoseptum, which were reduced in morphant embryos. Muscle fiber detachments were not observed in the F-actin immunofluorescent staining, suggesting that although the myoseptal attachments are present, they may be weaker. Taken together, these data suggest that inpp5ka is required for appropriate sarcomere assembly and function.

In summary, we identified five independent alleles in *INPP5K* leading to a disorder characterized by short
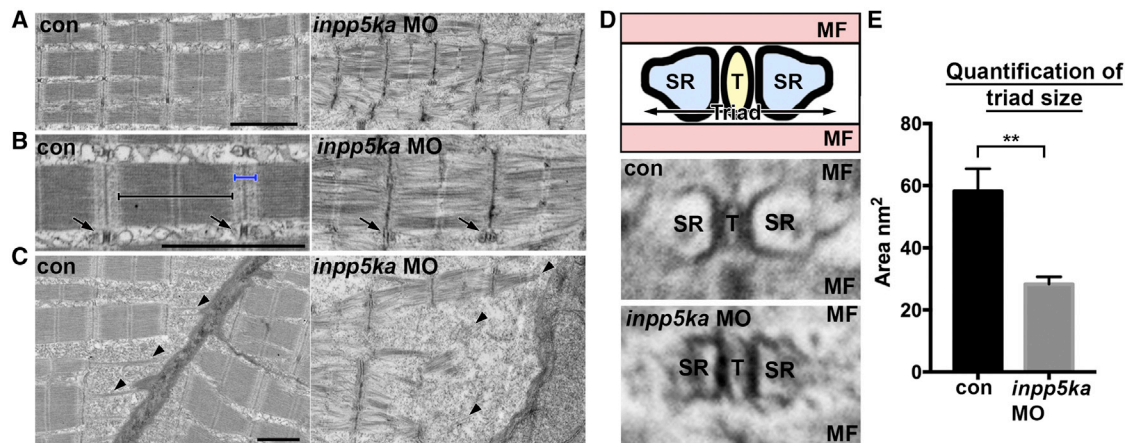
Figure 4. Zebrafish Loss of *inpp5ka* Results in Disorganized Myofibrils and Insufficient Sarcomere Assembly, as Analyzed by Transmission Electron Microscopy

(A) Assessment of sarcomere assembly at the ultrastructural level shows less compact myobrils, short sarcomere length, and undefined regional divisions. Scale bar represents 2 μm.

(B) High-magnification image of sarcomere assembly indicates the loss of defined anisotropic (black bracket) and isotropic (blue bracket) bands in morphant embryos. T-tubules are also notably smaller than control embryos (arrows). Scale bar represents 2 μm.

(C) Muscle fiber attachments at the somite borders presented disorganized and weak unions with the myoseptum in morphants embryos. Scale bar represents 1 μm.

(D) Top panel shows a schematic diagram of the Triad assembly, composed of the sarcoplasmic reticulum (SR) and T-tubule (T) sandwiched between muscle fibers (MF). Middle and lower panels show representative triad morphology for control and *inpp5ka* morphant fish, respectively.

(E) Triad size was quantified using the combined area of SR and T per triad. Con 58.2 ± SEM 7.254; n = 10, *inpp5ka*MO 28.3 ± SEM 2.371; n = 10. **p ≤ 0.01, as analyzed by an unpaired t test.

stature, ID, CMD, and cataracts. *inpp5k* loss-of-function modeling in the zebrafish led to a constellation of phenotypes that closely resembles the human presentation, including reduced growth, microcephaly, lens disorganization, reduced motility, and myopathy. The clinical presentation partially overlaps with MSS, and with at least two subjects showing a reduction in dystroglycan glycosylation, suggests a continuum with the dystroglycanopathies. This combination of phenotypes could be explained both by INPP5K enzymatic function and by its binding partners in the ER. Because of its role in converting PIP_2, INPP5K has been shown to promote myoblast differentiation by controlling the myogenic loop triggered by insulin-growth factor II (IGF-II) through the PI3K-AKT-mTOR pathway.[31] Little is known about the role of INPP5K in the brain, but IGF-II activity is also critical for learning and memory consolidation.[32] It is possible that changes in AKT-mTOR activity in the brain will contribute to cognitive deficits as this signaling pathway has been found disrupted in multiple neurodevelopmental disorders.[33] In addition, INPP5K's signaling activity is directly regulated by its binding partner HSPA5/BiP,[15,34] which is in turn regulated by the MSS-associated gene *SIL1*.[11] SIL1 regulates the activation stage of HSPA5/BiP in the ER and BiP is a critical chaperone for trafficking of glycoproteins.[11] Therefore, INPP5K could alter dystroglycan targeting by altering HSPA5/BiP function. Future studies must address the role of INPP5K in signaling regulation and glycoprotein trafficking during brain and muscle development.

Web Resources

ANNOVAR, http://annovar.openbioinformatics.org/en/latest/
Ensembl Genome Browser, http://www.ensembl.org/index.html
ExAC Browser, http://exac.broadinstitute.org/
FANTOM5, http://fantom.gsc.riken.jp/5/
GenBank, http://www.ncbi.nlm.nih.gov/genbank/
GME Variome, http://igm.ucsd.edu/gme
gnomAD Browser, http://gnomad.broadinstitute.org/
NCBI HomoloGene, http://www.ncbi.nlm.nih.gov/homologene
OMIM, http://www.omim.org/
PolyPhen-2, http://genetics.bwh.harvard.edu/pph2/
SIFT, http://sift.bii.a-star.edu.sg/
ZebSolutions, http://zebsolutions.co.uk/

References

1. Kang, P.B., Morrison, L., Iannaccone, S.T., Graham, R.J., Bönnemann, C.G., Rutkowski, A., Hornyak, J., Wang, C.H., North, K., Oskoui, M., et al.; Guideline Development Subcommittee of the American Academy of Neurology and the Practice Issues Review Panel of the American Association of Neuromuscular & Electrodiagnostic Medicine (2015). Evidence-based guideline summary: evaluation, diagnosis, and management of congenital muscular dystrophy: Report of the Guideline Development Subcommittee of the American Academy of Neurology and the Practice Issues Review Panel of the American Association of Neuromuscular & Electrodiagnostic Medicine. Neurology *84*, 1369–1378.

2. Bönnemann, C.G., Wang, C.H., Quijano-Roy, S., Deconinck, N., Bertini, E., Ferreiro, A., Muntoni, F., Sewry, C., Béroud, C., Mathews, K.D., et al.; Members of International Standard of Care Committee for Congenital Muscular Dystrophies (2014). Diagnostic approach to the congenital muscular dystrophies. Neuromuscul. Disord. *24*, 289–311.

3. Manzini, M.C., and Walsh, C.A. (2011). What disorders of cortical development tell us about the cortex: one plus one does not always make two. Curr. Opin. Genet. Dev. *21*, 333–339.

4. Mercuri, E., and Muntoni, F. (2012). The ever-expanding spectrum of congenital muscular dystrophies. Ann. Neurol. *72*, 9–17.

5. Wells, L. (2013). The o-mannosylation pathway: glycosyltransferases and proteins implicated in congenital muscular dystrophy. J. Biol. Chem. *288*, 6930–6935.

6. Mercuri, E., Messina, S., Bruno, C., Mora, M., Pegoraro, E., Comi, G.P., D'Amico, A., Aiello, C., Biancheri, R., Berardinelli, A., et al. (2009). Congenital muscular dystrophies with defective glycosylation of dystroglycan: a population study. Neurology *72*, 1802–1809.

7. Carss, K.J., Stevens, E., Foley, A.R., Cirak, S., Riemersma, M., Torelli, S., Hoischen, A., Willer, T., van Scherpenzeel, M., Moore, S.A., et al.; UK10K Consortium (2013). Mutations in GDP-mannose pyrophosphorylase B cause congenital and limb-girdle muscular dystrophies associated with hypoglycosylation of α-dystroglycan. Am. J. Hum. Genet. *93*, 29–41.

8. Senderek, J., Krieger, M., Stendel, C., Bergmann, C., Moser, M., Breitbach-Faller, N., Rudnik-Schöneborn, S., Blaschek, A., Wolf, N.I., Harting, I., et al. (2005). Mutations in SIL1 cause Marinesco-Sjögren syndrome, a cerebellar ataxia with cataract and myopathy. Nat. Genet. *37*, 1312–1314.

9. Krieger, M., Roos, A., Stendel, C., Claeys, K.G., Sonmez, F.M., Baudis, M., Bauer, P., Bornemann, A., de Goede, C., Dufke, A., et al. (2013). SIL1 mutations and clinical spectrum in patients with Marinesco-Sjogren syndrome. Brain *136*, 3634–3644.

10. Reinhold, A., Scheer, I., Lehmann, R., Neumann, L.M., Michael, T., Varon, R., and Von Moers, A. (2003). MR imaging features in Marinesco-Sjögren syndrome: severe cerebellar atrophy is not an obligatory finding. AJNR Am. J. Neuroradiol. *24*, 825–828.

11. Behnke, J., Feige, M.J., and Hendershot, L.M. (2015). BiP and its nucleotide exchange factors Grp170 and Sil1: mechanisms of action and biological functions. J. Mol. Biol. *427*, 1589–1608.

12. Gurung, R., Tan, A., Ooms, L.M., McGrath, M.J., Huysmans, R.D., Munday, A.D., Prescott, M., Whisstock, J.C., and Mitchell, C.A. (2003). Identification of a novel domain in two mammalian inositol-polyphosphate 5-phosphatases that mediates membrane ruffle localization. The inositol 5-phosphatase skip localizes to the endoplasmic reticulum and translocates to membrane ruffles following epidermal growth factor stimulation. J. Biol. Chem. *278*, 11376–11385.

13. Ijuin, T., Mochizuki, Y., Fukami, K., Funaki, M., Asano, T., and Takenawa, T. (2000). Identification and characterization of a novel inositol polyphosphate 5-phosphatase. J. Biol. Chem. *275*, 10870–10875.

14. Lizio, M., Harshbarger, J., Shimoji, H., Severin, J., Kasukawa, T., Sahin, S., Abugessaisa, I., Fukuda, S., Hori, F., Ishikawa-Kato, S., et al.; FANTOM consortium (2015). Gateways to the FANTOM5 promoter level mammalian expression atlas. Genome Biol. *16*, 22.

15. Ijuin, T., Hatano, N., and Takenawa, T. (2016). Glucose-regulated protein 78 (GRP78) binds directly to PIP3 phosphatase SKIP and determines its localization. Genes Cells *21*, 457–465.

16. Scott, E.M., Halees, A., Itan, Y., Spencer, E.G., He, Y., Azab, M.A., Gabriel, S.B., Belkadi, A., Boisson, B., Abel, L., et al.; Greater Middle East Variome Consortium (2016). Characterization of Greater Middle Eastern genetic variation for enhanced disease gene discovery. Nat. Genet. *48*, 1071–1076.

17. Lek, M., Karczewski, K.J., Minikel, E.V., Samocha, K.E., Banks, E., Fennell, T., O'Donnell-Luria, A.H., Ware, J.S., Hill, A.J., Cummings, B.B., et al.; Exome Aggregation Consortium (2016). Analysis of protein-coding genetic variation in 60,706 humans. Nature *536*, 285–291.

18. Kircher, M., Witten, D.M., Jain, P., O'Roak, B.J., Cooper, G.M., and Shendure, J. (2014). A general framework for estimating the relative pathogenicity of human genetic variants. Nat. Genet. *46*, 310–315.

19. Manzini, M.C., Tambunan, D.E., Hill, R.S., Yu, T.W., Maynard, T.M., Heinzen, E.L., Shianna, K.V., Stevens, C.R., Partlow, J.N., Barry, B.J., et al. (2012). Exome sequencing and functional validation in zebrafish identify GTDC2 mutations as a cause of Walker-Warburg syndrome. Am. J. Hum. Genet. *91*, 541–547.

20. Robinson, J.T., Thorvaldsdóttir, H., Winckler, W., Guttman, M., Lander, E.S., Getz, G., and Mesirov, J.P. (2011). Integrative genomics viewer. Nat. Biotechnol. *29*, 24–26.

21. Sobreira, N., Schiettecatte, F., Valle, D., and Hamosh, A. (2015). GeneMatcher: a matching tool for connecting investigators with an interest in the same gene. Hum. Mutat. *36*, 928–930.

22. Sobreira, N., Schiettecatte, F., Boehm, C., Valle, D., and Hamosh, A. (2015). New tools for Mendelian disease gene identification: PhenoDB variant analysis module; and GeneMatcher, a web-based tool for linking investigators with an interest in the same gene. Hum. Mutat. *36*, 425–431.

23. Ezgu, F., Krejci, P., Li, S., de Sousa, C., Graham, J.M., Jr., Hansmann, I., He, W., Porpora, K., Wand, D., Wertelecki, W., et al. (2014). Phenotype-genotype correlations in patients with Marinesco-Sjögren syndrome. Clin. Genet. *86*, 74–84.

24. Reed, U.C., Tsanaclis, A.M., Vainzof, M., Marie, S.K., Carvalho, M.S., Roizenblatt, J., Pedreira, C.C., Diament, A., and Levy, J.A. (1999). Merosin-positive congenital muscular dystrophy in two siblings with cataract and slight mental retardation. Brain Dev. *21*, 274–278.

25. Topaloğlu, H., Yetük, M., Talim, B., Akçören, Z., and Cağlar, M. (1997). Merosin-positive congenital muscular dystrophy with mental retardation and cataracts: a new entity in two families. Eur. J. Paediatr. Neurol. *1*, 127–131.

26. Howe, K., Clark, M.D., Torroja, C.F., Torrance, J., Berthelot, C., Muffato, M., Collins, J.E., Humphray, S., McLaren, K., Matthews, L., et al. (2013). The zebrafish reference genome sequence and its relationship to the human genome. Nature *496*, 498–503.

27. Lynch, M., and Conery, J.S. (2000). The evolutionary fate and consequences of duplicate genes. Science *290*, 1151–1155.

28. Greiling, T.M.S., and Clark, J.I. (2009). Early lens development in the zebrafish: a three-dimensional time-lapse analysis. Dev. Dyn. *238*, 2254–2265.

29. Paolini, C., Quarta, M., Nori, A., Boncompagni, S., Canato, M., Volpe, P., Allen, P.D., Reggiani, C., and Protasi, F. (2007). Reorganized stores and impaired calcium handling in skeletal muscle of mice lacking calsequestrin-1. J. Physiol. *583*, 767–784.

30. Gupta, V., Kawahara, G., Gundry, S.R., Chen, A.T., Lencer, W.I., Zhou, Y., Zon, L.I., Kunkel, L.M., and Beggs, A.H. (2011). The zebrafish dag1 mutant: a novel genetic model for dystroglycanopathies. Hum. Mol. Genet. *20*, 1712–1725.

31. Ijuin, T., and Takenawa, T. (2012). Role of phosphatidylinositol 3,4,5-trisphosphate (PIP3) 5-phosphatase skeletal muscle- and kidney-enriched inositol polyphosphate phosphatase (SKIP) in myoblast differentiation. J. Biol. Chem. *287*, 31330–31341.

32. Chen, D.Y., Stern, S.A., Garcia-Osta, A., Saunier-Rebori, B., Pollonini, G., Bambah-Mukku, D., Blitzer, R.D., and Alberini, C.M. (2011). A critical role for IGF-II in memory consolidation and enhancement. Nature *469*, 491–497.

33. Lipton, J.O., and Sahin, M. (2014). The neurology of mTOR. Neuron *84*, 275–291.

34. Ijuin, T., Hatano, N., Hosooka, T., and Takenawa, T. (2015). Regulation of insulin signaling in skeletal muscle by PIP3 phosphatase, SKIP, and endoplasmic reticulum molecular chaperone glucose-regulated protein 78. Biochim. Biophys. Acta *1853*, 3192–3201.